Macrophage migration inhibitory factor knockout attenuates endotoxin-induced cardiac dysfunction in mice

Jie Zhang[1], Xin Zhang[2], Yuqi Cui[3], Lianqun Cui[3], Peng Zhao[3]

[1]Department of Nutrition, Shandong Provincial Hospital affiliated to Shandong University, Jinan, China
[2]Department of Radiology, Police General Hospital of Shandong Province, Jinan, China
[3]Department of Cardiology, Shandong Provincial Hospital affiliated to Shandong University, Jinan, China

A b s t r a c t

Background: Accumulated evidence suggests that macrophage migration inhibitory factor (MIF) plays a key role not only in acute and chronic inflammatory diseases but also in cardiovascular disease. The cardiac dysfunction is related to lipopolysaccharide (LPS) in sepsis.

Aim: This study was designed to examine whether MIF mediates LPS-induced cardiac dysfunction and address the mechanisms.

Methods: Echocardiography, immunohistochemical analysis, cell shortening/re-lengthening, and intracellular Ca^{2+} fluorescence evaluation were performed in whole hearts and isolated cardiomyocytes from C57 and MIF knockout mice treated with or without LPS. Reactive oxygen species and protein carbonyl formation were measured. Activation of mitogen-activated protein kinases and endoplasmic reticulum stress markers were evaluated using Western blot analysis. Human umbilical vein endothelial cells (HUVECs) were transfected with lentiviruses carrying short hairpin RNA (shRNA) to inhibit MIF.

Results: Echocardiography revealed that cardiac function was impaired and macrophage infiltration was increased in LPS-treated C57 mice. Peak shortening and maximal velocity of shortening/re-lengthening were significantly reduced and the duration of re-lengthening was prolonged in LPS-treated C57 mice. Reactive oxygen species and protein carbonyl levels were increased in LPS-treated C57 mice. These dysfunctional changes were attenuated in MIF knockout mice that were challenged with LPS. Western blot analysis revealed that activated p-JNK, p-ERK, and endoplasmic reticulum stress protein marker expression was decreased in LPS-treated MIF knockout mice. p-ERK and p-JNK levels were knocked down in MIF shRNA-transfected HUVECs.

Conclusions: The data collectively suggest that MIF mediates LPS-induced cardiac dysfunction in murine cardiomyocytes, which was attenuated by MIF knockout, and the therapeutic option with regard to MIF may aid the management of cardiac dysfunction in sepsis.

Key words: macrophage migration inhibitory factor, sepsis, cardiac dysfunction

Kardiol Pol 2018; 76, 5: 871–880

INTRODUCTION

Sepsis is one of the main causes of death among hospitalised patients, especially those in the intensive care unit. It is a major medical problem that often results in multiple organ failure. Sepsis is known to be triggered by the effects of one or more components of the invading microorganisms, including lipopolysaccharide (LPS) endotoxin from gram-negative bacteria, which results in systemic disruption of the normal inflammatory response [1, 2]. Heart failure is the most devastating organ dysfunction arising from septic shock. The relationship between myocardial dysfunction and cardiovascular failure in human and experimental septic shock has become clearer. A series of clinical cardiac manifestations are commonly observed in septic patients, including biventricular dilatation, decreased ejection fraction, and decreased myocardial contractility.

Many studies have shown the activation of multiple stress signalling cascades in sepsis. Inducible nitric oxide synthase (iNOS), oxidative stress, and mitogen-activated protein kinase (MAPK) are believed to play a pivotal role in the pathogenesis of septic cardiac dysfunction [3–5]. Reactive oxygen species (ROS) are formed as a natural by-product of the normal metabolism of oxygen and play important roles in cell signalling and homeostasis. Extracellular signal-related kinase (ERK) and c-Jun N-terminal kinase (JNK) are major MAPK family members. A variety of stimuli can lead to the accumulation of unfolded and misfolded proteins in the endoplasmic reticulum (ER). The unfolded protein response (UPR) initiates ER stress when ER transmembrane sensors detect the accumulation of unfolded proteins.

Macrophage migration inhibitory factor (MIF) was originally discovered as a lymphokine derived from activated T cells. MIF inhibits the random migration of macrophages in vitro and regulates T-cell activation as well as proliferation. Proinflammatory actions of MIF have been reported in various inflammatory diseases, such as sepsis, rheumatoid arthritis, and atherosclerosis [6–8]. Ha et al. [9] treated caecal ligation and puncture-induced septic mice with glucan phosphate, which has been reported to modulate innate immunity and proinflammatory signalling in sepsis, and showed that cardiac function was preserved and MIF expression was attenuated. Furthermore, patients with rapidly fatal outcomes exhibited simultaneously high MIF and interleukin (IL)-10 levels in the early phase of severe sepsis [10]. Nonetheless, little information is available regarding the role of MIF in cardiac dysfunction due to sepsis. This study aimed to verify the contribution of MIF to myocardial dysfunction and address the possible mechanisms.

METHODS

Experimental animals and LPS treatment. All animal procedures were approved by the Animal Care and Use Committee at the Shandong Provincial Hospital affiliated to Shandong University (Shandong, China). Age-matched male C57 and MIF knockout mice (MIFKO) on a C57 background were used. There were eight mice in each experimental group. All animals were kept in our institutional animal facility with free access to laboratory chow and tap water. On the day of experimentation, both C57 and MIFKO mice were intraperitoneally injected with 4 mg/kg *Escherichia Coli* LPS (Sigma-Aldrich, St. Louis, MO, USA) dissolved in sterile saline or an equivalent volume of pathogen-free saline (for control groups). The dosage for LPS injection was chosen based on previous studies to induce overt myocardial dysfunction without significant mortality [11]. Four hours after LPS challenge, mice were anaesthetised using ketamine and xylazine (3:5, 1.32 mg/kg), and were sacrificed by cervical dislocation.

Cell culture and gene interference. Human umbilical vein endothelial cells (HUVECs) were purchased from the ATCC (CRL-1730) and cultured in Dulbecco's Modified Eagle's Medium containing 10% foetal bovine serum, 100 U/mL penicillin, 100 U/mL streptomycin, and L-glutamine at 37°C in 5% CO_2. shRNA was synthesised by Genechem (Shanghai, China). HUVECs were transfected with lentiviruses carrying shRNAs against MIF. To achieve stable interference, duplex RNAs targeting MIF (sense strand: CCAGTACATCGCGGTGCACGT) and control RNAs (sense strand: TTCTCCGAACGTGTCACGT) were inserted into the GV115 vector according to the manufacturer's instructions. The control cells and knockdown cells were treated with 100 ng/mL LPS for the indicated times.

Histological and immunohistochemical analysis. Hearts from mice were collected at the indicated times, fixed overnight in 10% formalin, and embedded in paraffin. Serial 5-μm heart sections from each group were analysed. Samples were stained with haematoxylin and eosin for routine histologic examination. The histological sections were stained with primary antibodies against α-2-macroglobulin (Mac-2) (1:200, Abcam, Cambridge, MA, USA) at 4°C overnight. The bound antibodies were labelled using a secondary antibody (VECTOR Laboratories, Inc., Burlingame, CA, USA). Images were analysed with NIH ImageJ software. The number of Mac-2-positive macrophages was counted blindly and expressed as a percentage of the total number of cardiomyocytes in five sequentially cut 5-μm sections of each heart.

Echocardiographic examination. Transthoracic echocardiography was performed on animals using a Sequoia 512 device with a GE-i13L probe before they were sacrificed. Isoflurane (1.5%–2.0%) was used for anaesthesia. The M-mode echocardiogram was obtained in the short-axis view of the left ventricle at the level of the *chordae tendineae*. Left ventricular end-diastolic dimension (LVEDD), left ventricular end-systolic dimension (LVESD), and left ventricular diastolic interventricular septal thickness were measured. Left ventricular ejection fraction (LVEF) was also calculated from M-mode echocardiograms. Data from three to five consecutive cardiac cycles were analysed and averaged.

Isolation of murine cardiomyocytes. Mice were given 100 units of heparin intraperitoneally (Sagent Pharmaceuticals, Schaumburg, IL, USA) for anticoagulation. The heart was excised and fastened onto a heart perfusion apparatus (Radnoti, Monrovia, CA, USA), and perfusion was initiated in the Langendorff system. Hearts were perfused at 37°C with a Ca^{2+}-free Krebs-Henseleit-based buffer (pH 7.3). After a few minutes of stabilisation, the heart was digested with the same perfusion buffer containing 0.067 mg/mL of Liberase Blendzyme 4 (Roche, Indianapolis, IN, USA). After perfusion, the left ventricles were removed and minced to disperse cardiomyocytes in Ca^{2+}-free KHB buffer. Extracellular Ca^{2+} was incrementally added to achieve a concentration of 1.25 mM. Only rod-shaped myocytes with clear edges were selected for mechanical and intracellular Ca^{2+} transient studies. Cells were used for functional or biochemical assessment within 6 h of isolation.

Table 1. Heart weight and echocardiographic parameters of lipopolysaccharide (LPS)-treated C57 and migration inhibitory factor knockout (MIFKO) mice

Parameter	C57	C57-LPS	MIFKO	MIFKO-LPS
Heart weight [mg]	115 ± 9	123 ± 18	119 ± 13	118 ± 10
Heart rate [bpm]	422 ± 39	441 ± 21	449 ± 30	430 ± 26
IVS thickness [mm]	0.90 ± 0.03	0.88 ± 0.05	0.87 ± 0.08	0.79 ± 0.06
LVEDD [mm]	2.27 ± 0.14	2.40 ± 0.21	2.16 ± 0.28	2.29 ± 0.19
LVESD [mm]	1.11 ± 0.12	1.79 ± 0.13*	1.19 ± 0.11	1.39 ± 0.15
Ejection fraction [%]	71.5 ± 5.2	47.7 ± 5.8*	68.7 ± 7.1	58.8 ± 4.9#

Data are shown as mean ± standard error of the mean (SEM); IVS — interventricular septal; LVEDD — left ventricular end-diastolic dimension; LVESD — left ventricular end-systolic dimension; n = 4–6 mice per group. *$p < 0.05$ vs. the C57 group; #$p < 0.05$ vs. the C57-LPS group

Cell shortening/re-lengthening. IonOptix SoftEdge software (Westwood, MA, USA) was used to capture changes in cell length during shortening and re-lengthening. Cell shortening and re-lengthening were assessed using the following indices: peak shortening (PS) — indicative of the maximal amplitude a cell can shorten during contraction; maximal velocities of cell shortening/re-lengthening ($\pm$ dL/dt) — indicative of peak ventricular contractility; time-to-PS (TPS) — indicative of systolic duration; time-to-90% re-lengthening (TR_{90}) — indicative of diastolic duration (90% rather than 100% re-lengthening was used to avoid the noisy signal at the baseline concentration); and maximal velocities of shortening/re-lengthening — indicative of maximal velocities of ventricular pressure increases/decreases [4].

Intracellular Ca²⁺ fluorescence measurement. Intracellular Ca²⁺ was measured using a dual-excitation, single-emission photomultiplier system (IonOptix Corporation, Milton, MA, USA). Cardiomyocytes were loaded with Fura-2-AM ($2\,\mu M$) and were exposed to light emitted by a 75-W halogen lamp through either a 340-nm or 380-nm filter while being stimulated to contract at a frequency of 0.5 Hz. Fluorescence emissions were then detected. The fluorescence decay time was assessed as an indication of intracellular Ca²⁺ clearing. Both single and bi-exponential curve fit programmes were applied to calculate the intracellular Ca²⁺ decay constant [4].

Generation of intracellular ROS. The OxiSelect™ ROS Assay Kit (Cell Biolabs, CA, USA) is a cell-based assay that measures ROS activity. The assay employs the cell-permeable fluorogenic probe DCFH-DA, which diffuses into cells and is deacetylated by cellular esterases into a non-fluorescent form. In the presence of ROS, DCFH is rapidly oxidised to highly fluorescent DCF. The fluorescence signal was detected on a standard fluorometric plate reader.

Protein carbonyl assay. The protein carbonyl content in tissue lysate was determined using a Protein Carbonyl Colorimetric Assay Kit (Cell Biolabs, CA, USA) according to the manufacturer's instructions.

Western blot analysis. Cardiac tissue was sonicated in lysis buffer and centrifuged at 12,000 g for 10 min. Equal amounts ($20\,\mu g$) of protein and a pre-stained molecular weight marker were separated using 7% to 15% SDS-polyacrylamide gels in a minigel apparatus (Mini-PROTEAN II, Bio-Rad, Hercules, CA, USA) and were then transferred to nitrocellulose membranes (0.2-μm pore size, Bio-Rad). Membranes were blocked for 1 h in 5% non-fat milk before being rinsed in Tris Buffered Saline-Tween. The membranes were incubated overnight at 4°C with anti-ERK, anti-phospho-ERK (p-ERK), anti-JNK, anti-phospho-JNK (p-JNK), anti-IRE1α, anti-eIF2α, anti-Grp78, and anti-Gadd153 antibodies. Anti-ERK and anti-pERK antibodies were purchased from Santa Cruz Biotechnology (Santa Cruz, CA, USA). All other antibodies were acquired from Cell Signaling Technology (Beverly, MA, USA). After incubation with the primary antibodies, blots were incubated with horseradish peroxidase (HRP)-coupled anti-rabbit secondary antibodies (Cell Signaling, Beverly, MA, USA). Films were scanned with the Bio-Rad GS-700 scanner, and the relative density of the bands on the film was determined using ImageJ software.

Statistical analysis

Data are presented as the mean ± standard error of the mean (SEM) and analysed using GraphPad Prism 7.0 (La Jolla, CA, USA) statistical analysis software. Differences were assessed using analysis of variance (ANOVA) followed by Tukey's post hoc test. A p value < 0.05 was considered statistically significant.

RESULTS
Heart weight and echocardiographic properties of C57 and MIFKO mice treated with LPS

Lipopolysaccharide treatment did not affect heart weights in either C57 or MIFKO mice. Knockout of MIF did not affect heart rate, interventricular septal thickness, LVEDD, LVESD, or LVEF. LPS significantly increased LVESD and reduced ejection fraction in LPS-treated C57 mouse hearts, the effect of which was attenuated or ablated by MIF knockout (Table 1, Fig. 1).

Inflammation in LPS-treated mice

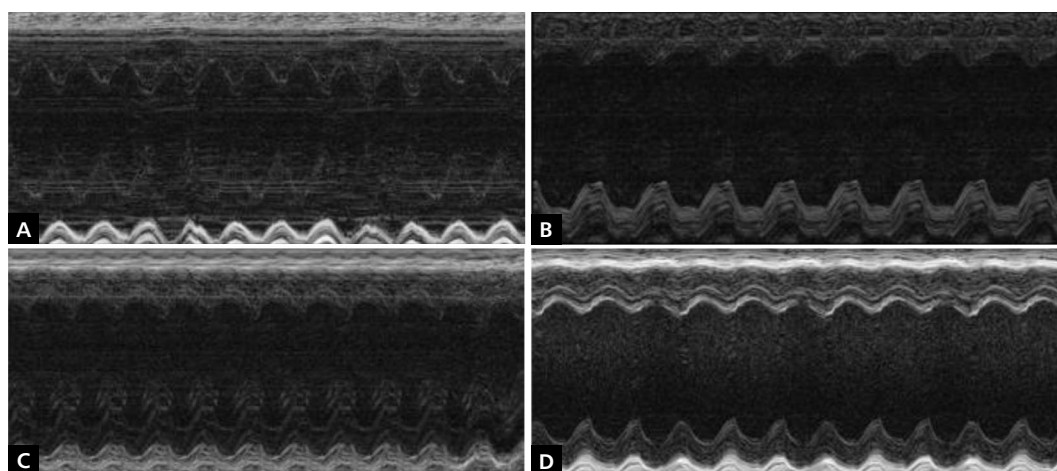The effect of MIF knockout on cardiac inflammation was assessed by immunohistochemical staining with an antibody

Figure 1. Representative echocardiographic recordings from four mouse groups. **A.** The C57 group; **B.** The C57-LPS group; **C.** The MIFKO group; **D.** The MIFKO-LPS group
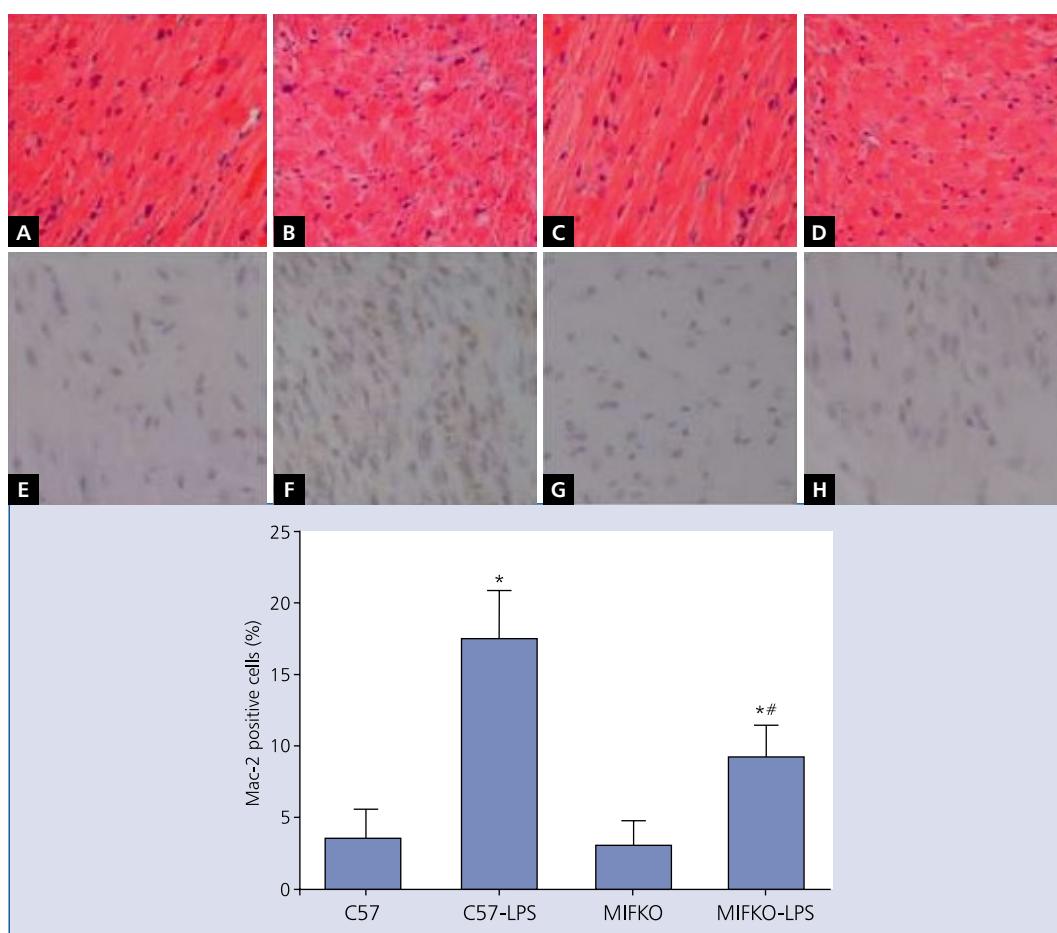

Figure 2. Representative images of haematoxylin and eosin staining and Mac-2 staining for the evaluation of inflammation. **A, E.** The C57 group; **B, F.** The C57-LPS group; **C, G.** The MIFKO group; **D, H.** The MIFKO-LPS group. Data are shown as mean ± standard error of the mean (SEM); n = 4 samples per group; *p < 0.05 vs. the C57 group; #p < 0.05 vs. the C57-LPS group

against Mac-2 (a macrophage marker). Macrophage infiltration was unchanged in MIF knockout mice. More inflammatory cells infiltrated the hearts of LPS-treated C57 mice compared to the hearts of their littermates. In LPS-treated MIFKO mice, Mac-2-positive cell number was decreased compared with LPS-treated C57 mice (Fig. 2).
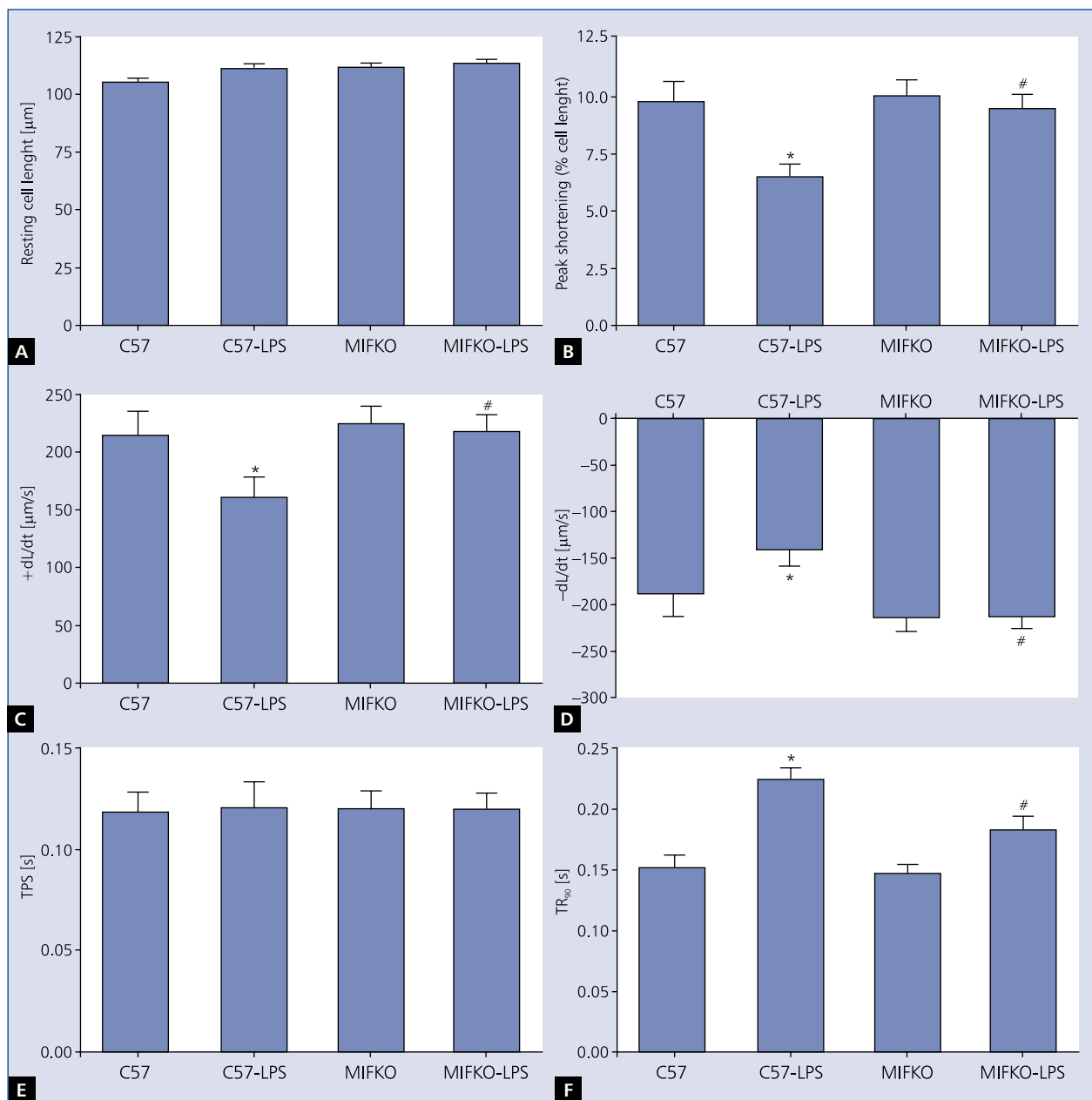
Figure 3. Cardiomyocyte contractile properties in C57 and MIFKO mice treated with or without lipopolysaccharide (LPS) (4 mg/kg, i.p.). **A.** Resting cell length; **B.** Peak shortening (PS, normalised to cell length); **C.** Maximal velocity of shortening (+ dL/dt); **D.** Maximal velocity of re-lengthening (– dL/dt); **E.** Time to PS (TPS); **F.** Time to 90% re-lengthening (TR$_{90}$). Data are shown as mean ± standard error of the mean (SEM); n = 60 cells from three mice per group. *p < 0.05 vs. the C57 group; #p < 0.05 vs. the C57-LPS group

Mechanical and intracellular Ca²⁺ properties of murine cardiomyocytes

Mechanical recording revealed that the resting cell length was similar in cardiomyocytes from both C57 and MIFKO mouse hearts. However, cardiomyocytes from the LPS-treated C57 mice displayed significantly reduced PS and ± dL/dt associated with prolonged TR$_{90}$ and normal TPS. Interestingly, MIF knockout effectively protected cardiomyocytes from LPS-induced mechanical dysfunction without eliciting any overt side effects (Fig. 3), which indicated that MIFKO may play a protective role against LPS-induced cardiac dysfunction. To explore the potential mechanisms involved in the MIFKO-elicited protection against LPS-induced cardiomyocyte contractile defects, intracellular Ca²⁺ homeostasis was evaluated using the fluorescent dye fura-2. The results showed that a reduced intracellular Ca²⁺ clearance rate (i.e. increased decay
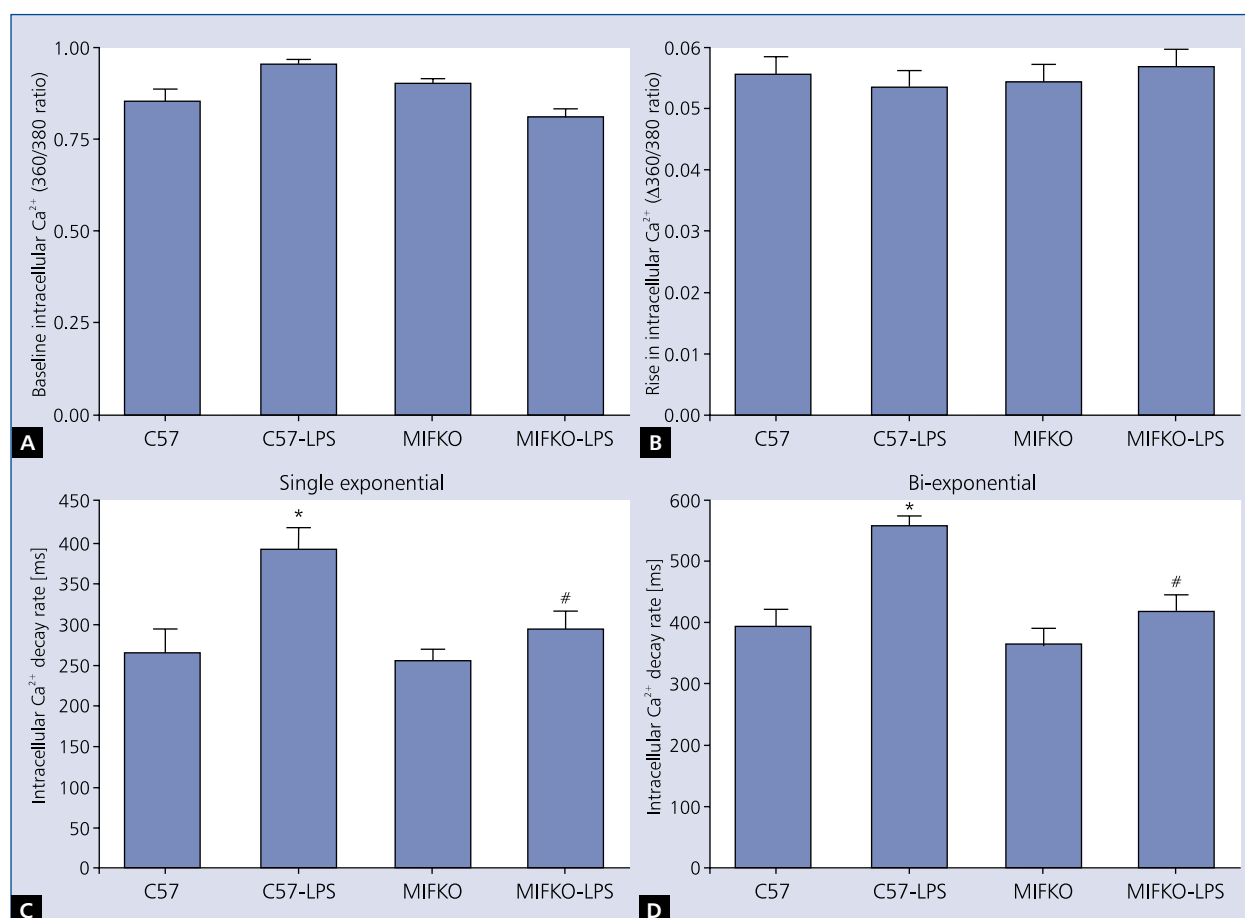
Figure 4. Intracellular Ca^{2+} properties in cardiomyocytes from C57 and MIFKO mice treated with or without lipopolysaccharide (LPS) (4 mg/kg, i.p.). **A.** Resting intracellular Ca^{2+}; **B.** Electrically stimulated rise in intracellular Ca^{2+}; **C, D.** Single- and bi-exponential intracellular Ca^{2+} decay rate. Data are shown as mean ± standard error of the mean (SEM); n = 60 cells from three mice per group. *$p < 0.05$ vs. the C57 group; #$p < 0.05$ vs. the C57-LPS group

time) (both single- and bi-exponential decay) was associated with unchanged resting and electrically stimulated increases in intracellular Ca^{2+} levels in the cardiomyocytes. Intriguingly, cardiomyocytes from LPS-treated C57 mice exhibited slower Ca^{2+} clearing than cardiomyocytes from LPS-treated MIFKO (Fig. 4). Together, these data suggest a beneficial role for MIF inhibition in LPS-associated cardiac dysfunction.

Effect of LPS on ROS generation and protein carbonyl formation

As shown in Figure 5A, ROS production was enhanced in myocytes from LPS (20 μg/mL)-treated mice. Interestingly, myocytes obtained from MIFKO mice displayed significantly reduced ROS generation in response to LPS exposure compared with those from LPS-treated C57 mice, suggesting that MIFKO partly antagonised LPS-induced ROS generation. These data indicate that the MIF inhibition may eliminate LPS-induced cardiac mechanical dysfunction via a mechanism related to reduction in ROS generation. The results shown

in Figure 5B indicate that protein carbonyl formation was enhanced in hearts from LPS-treated C57 mice compared with hearts from MIFKO mice. Although MIF knockout itself had little effect on cardiac protein carbonyl formation, it partially reversed LPS-induced protein carbonyl formation, suggesting a protecting effect of MIF deficiency against cardiac protein damage.

Effect of MIFKO on the LPS-induced activation of stress signalling

Lipopolysaccharide challenge is usually associated with activation of stress signalling. The results shown in Figure 6A, B demonstrate the activation of p-JNK and p-ERK in the myocardium following LPS challenge. This effect was attenuated in MIFKO mice. It is interesting that in MIFKO mice without LPS challenge the ratios of p-ERK/ERK and p-JNK/JNK were increased, whereas protein expression of non-phosphorylated ERK and JNK was not different between C57 and MIFKO mice. To further detect the effect of MIF knockdown on ERK and
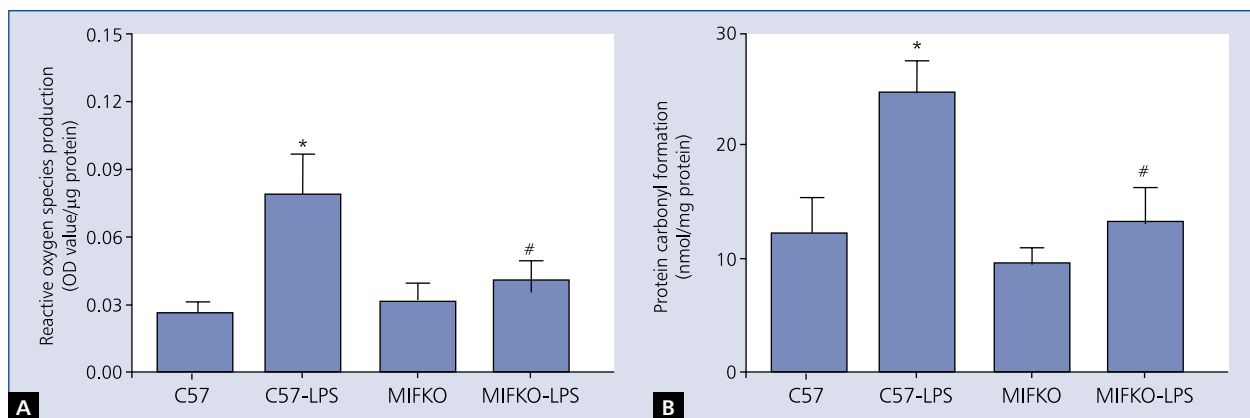
Figure 5. **A.** Intracellular reactive oxygen species measurement by dichlorofluorescein fluorescence detection; **B.** Protein damage evaluated by protein carbonyl formation. Data are shown as mean ± standard error of the mean (SEM); n = 4 samples per group. *p < 0.05 vs. the C57 group; #p < 0.05 vs. the C57-LPS group
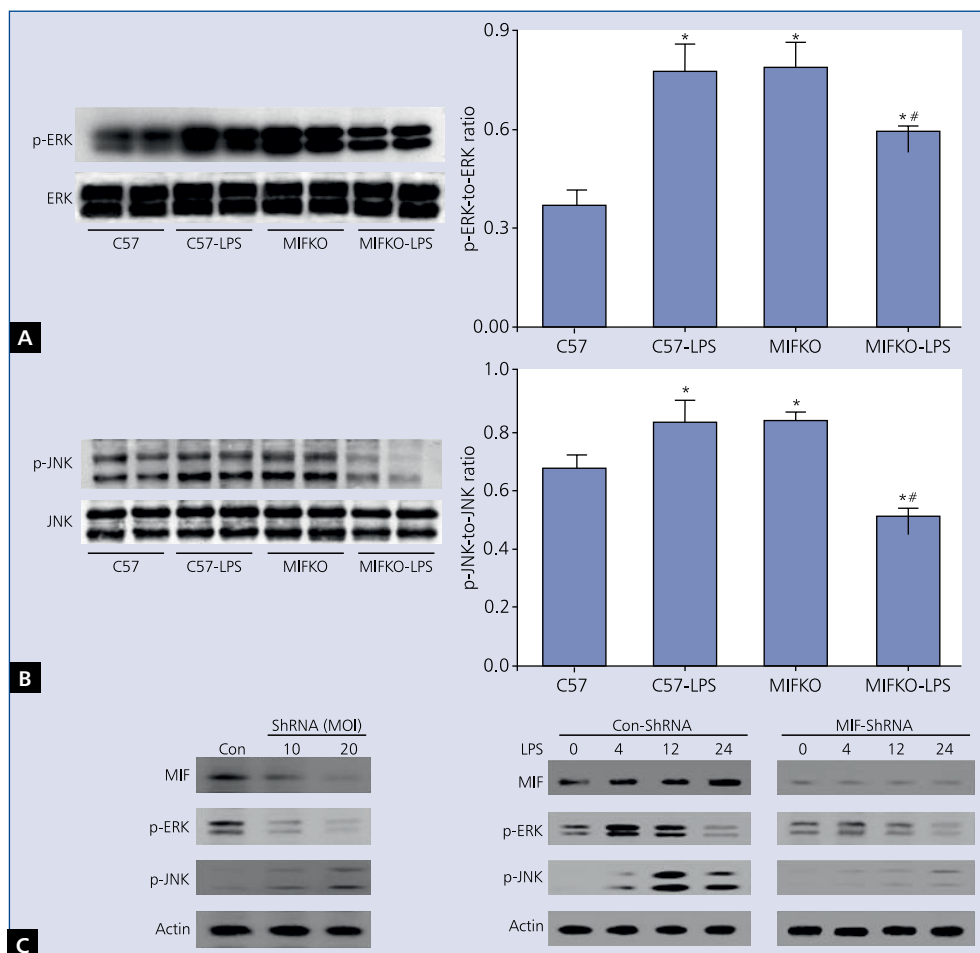

Figure 6. Western blot analysis exhibiting phosphorylation of extracellular signal-related kinase (ERK) and c-Jun N-terminal kinase (JNK) in the myocardium of C57 and MIFKO mice treated with or without lipopolysaccharide (LPS) (4 mg/kg. i.p.). **A.** The pJNK--to-JNK ratio; **B.** The pERK-to-ERK ratio. Data are shown as mean ± standard error of the mean (SEM); n = 4 samples per group. *p < 0.05 vs. the C57 group; #p < 0.05 vs. the C57-LPS group. The effect of migration inhibitory factor (MIF) knockdown on related signal transduction pathways; **C.** Human umbilical vein endothelial cells (HUVECs) were transfected with lentiviruses carrying MIF shRNA at different multiplicities of infection (MOIs) for 24 h. MIF, p-ERK, p-JNK, and actin levels were evaluated by Western blot; **D.** The control cells and knockdown cells were treated with 100 ng/mL LPS for 0, 4, 12, and 24 h. The effect of LPS on the expression of MIF, p-ERK, p-JNK, and actin was demonstrated by Western blot
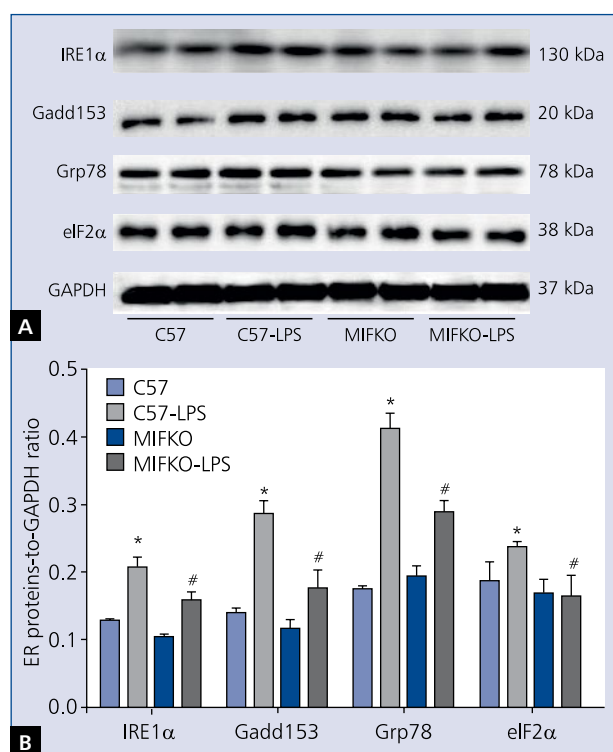
Figure 7. Western blot analysis of the expression of the endoplasmic reticulum (ER) stress markers IRE1α, Gadd153, Grp78, and eIF2α in the myocardium from C57 and MIFKO mice treated with or without lipopolysaccharide (LPS) (4 mg/kg, i.p.). **A.** Representative gel blots depicting IRE1α, Gadd153, Grp78, and eIF2α proteins expression as detected using specific antibodies; **B.** Pooled data of IRE1α, Gadd153, Grp78, and eIF2α proteins (normalised to GAPDH). Data are shown as mean ± standard error of the mean (SEM); n = 4 samples per group. *p < 0.05 vs. the C57 group; #p < 0.05 vs. the C57-LPS group

JNK, HUVECs were transfected with lentiviruses carrying MIF shRNA at different multiplicities of infection for 24 h. Figure 6C shows that p-ERK level was decreased by MIF shRNA transfection. However, p-JNK level was increased by MIF shRNA transfection. Control cells and MIF knockdown cells were treated with 100 ng/mL LPS for 0, 4, 12, and 24 h. LPS induced the expressions of MIF, p-ERK, and p-JNK, which were attenuated in MIF knockdown cells (Fig. 6D). p-JNK level at 24 h was increased by LPS treatment both in control cells and MIF knockdown cells comparing with its level at 0 h. This result was in accordance with the variation trend of p-JNK expression in Figure 6C.

Effect of MIFKO on LPS-induced ER stress

To further understand the molecular mechanism underlying the beneficial effects of MIFKO in the heart during LPS challenge, ER stress proteins were assessed by immunoblotting. The data clearly demonstrate that LPS markedly stimulated ER stress markers IRE1α, Gadd153, Grp78, and eIF2α in LPS-treated C57 mice (Fig. 7), the effect of which was obliterated by MIFKO. However, the baseline expression of IRE1α, Gadd153, Grp78, and eIF2α was unaffected by MIF knockout.

DISCUSSION

Our study revealed that cardiac knockout of MIF rescued LPS-induced cardiac contractile and intracellular Ca^{2+} dysfunction. Reactive oxygen species and protein carbonyl levels were decreased in LPS-treated MIFKO mice. The MIFKO-induced cardioprotection against sepsis may be attributed to the alleviation of ER stress in MIFKO mice. Furthermore, in MIFKO mice, the LPS-induced activation of JNK and ERK signalling molecules was decreased. More inflammatory cells infiltrated the hearts of LPS-treated C57 mice compared to those of LPS-treated MIFKO mice. Examination of mechanical properties revealed reduced PS, ± dL/dt, as well as prolonged relaxation duration (TR$_{90}$) in septic C57 cardiomyocytes. LPS treatment significantly attenuated cardiomyocyte contraction and the electrically stimulated rise in intracellular Ca^{2+}, suggesting a role for intracellular Ca^{2+} in endotoxin-induced cardiomyocyte dysfunction. Collectively, these findings suggest that MIF inhibition has a direct cardioprotective effect rather than an indirect effect, from the modulation of the LPS-induced endotoxin response. Data also showed that MIF inhibition itself did not significantly affect cardiac contractile function without the presence of endotoxin. The protective effect of MIF inhibition against LPS-induced cardiac dysfunction and ER stress implies its therapeutic potential in the clinic. Therefore, MIF inhibition may be used to manage cardiovascular complications in sepsis.

Migration inhibitory factor has been recognised as a potent proinflammatory mediator in the progression of systemic inflammation. This cytokine appears to be a critical regulator of the inflammatory pathways [12]. An abundance of clinical and experimental evidence has shown cardiac contractile dysfunction in sepsis. Animal studies have shown that administration of neutralising anti-MIF antibodies or deletion of the MIF gene protected mice from lethality induced by endotoxaemia or sepsis. Dhanantwari et al. [13] used cultured cardiomyocytes to determine whether MIF-induced contractile dysfunction was mediated in part by myocyte apoptosis and to identify MIF-activated intracellular signalling pathways in this process. MIF stimulated the rapid, transient phosphorylation of the stress kinases, p38 MAPK and JNK. This effect was attenuated by inactivation of MIF with the chemical inhibitor ISO-1. However, Xu et al. [14] showed that doxorubicin-induced cardiac remodelling and dysfunction were accentuated by genetic MIF deficiency, as shown by more pronounced adverse effects on mortality, and myocardial geometry and function. Many studies have shown the prospects of using anti-MIF antibodies in basic research and clinical applications. The inhibition of MIF may cause the reduction of the severity of age-related osteoarthritis in mice [15].

Targeted deletion of MIF gene delays the development of chronic lymphocytic leukaemia and prolongs survival in mice [16].

Mitogen-activated protein kinase pathways can be activated by cellular stress signals, such as inflammatory cytokines. ERK, JNK, and p38 are major MAPK family members and play a vital role in myocardial injury by promoting cardiomyocyte apoptosis and inflammation [17]. Our results demonstrated that MIFKO ablated the sepsis-elicited activation of ERK and JNK. Lin et al. [18] showed that MIF was produced in the lungs and released into circulation during experimental sepsis and that this release was temporally related to activation of the stress-related MAPK signalling pathways in the myocardium. The data from Aoki et al. [19] showed that MIF activated JNK and p38, although JNK has been shown to be a direct activator of mitochondrial death machinery in cardiomyocytes. Recently, a study showed that compared to WT mice, MIFKO mice had a significantly lower incidence of post-MI cardiac rupture and exhibited amelioration of cardiac remodelling. These effects were associated with suppressed myocardial leukocyte infiltration, inflammatory mediator expression, and MMP-2, MMP-9, p38, and JNK activity [20].

The endoplasmic reticulum is an extensive intracellular membranous network involved in Ca^{2+} storage, Ca^{2+} signalling, glycosylation, and trafficking of membrane and secretory proteins. Our results revealed overt ER stress in the myocardium following LPS-induced endotoxaemia. ER stress has been shown to contribute to neurodegenerative disorders and ischaemia reperfusion-induced cardiac damage [21, 22]. Our data revealed upregulated expression of the ER chaperone Grp78, which directly interacts with all three ER stress sensors, eIF2α, Gadd153, and IRE1α in sepsis. Upregulation of Grp78 is pivotal for cell survival because it facilitates the folding and assembly of ER proteins and prevents them from aggregating during ER stress. We observed that the LPS-induced increase of Grp78, Gadd153, eIF2α, and IRE1α was attenuated in MIFKO mice, which suggests an important role for MIF in ER stress induction in the heart.

Three limitations of this study should be mentioned. First, the dose of LPS used to induce sepsis in mice is much higher than that observed in humans. Additionally, different genes are expressed in sepsis in mice and humans. The innate immune system can be activated in sepsis, and it can exert both positive and negative impacts upon the organism. Second, long-term observations are required to confirm whether the response of ER stress is a "double-edged sword" for cardiac function. Third, specimens and data should be collected from septic patients to observe the relationship between cardiac function and sepsis in the clinic.

In conclusion, our study revealed that the cardiac knockout of MIF rescued LPS-induced cardiomyocyte contractile dysfunction and intracellular Ca^{2+} mishandling, potentially by alleviating stress signalling activation. The sequential

relationship between MIF and ER stress in altering cardiac function remains to be determined. Whether ER stress is adaptive or maladaptive in the context of sepsis also remains to be determined. These approaches are essential for the potential application of anti-MIF in the clinical management of endotoxin-associated cardiac dysfunction.

Conflict of interest: *none declared*

References

1. Oliva M, Rullan AJ, Piulats JM. Uveal melanoma as a target for immune-therapy. Ann Transl Med. 2016; 4(9): 172, doi: 10.21037/atm.2016.05.04, indexed in Pubmed: 27275485.
2. Kim KW, Kim HR. Macrophage migration inhibitory factor: a potential therapeutic target for rheumatoid arthritis. Korean J Intern Med. 2016; 31(4): 634–642, doi: 10.3904/kjim.2016.098, indexed in Pubmed: 27169879.
3. Zhang LB, Man ZT, Li W, et al. Calcitonin protects chondrocytes from lipopolysaccharide-induced apoptosis and inflammatory response through MAPK/Wnt/NF-κB pathways. Mol Immunol. 2017; 87: 249–257, doi: 10.1016/j.molimm.2017.05.002, indexed in Pubmed: 28514714.
4. Zhao P, Turdi S, Dong F, et al. Cardiac-specific overexpression of insulin-like growth factor I (IGF-1) rescues lipopolysaccharide-induced cardiac dysfunction and activation of stress signaling in murine cardiomyocytes. Shock. 2009; 32(1): 100–107, doi: 10.1097/SHK.0b013e31818ec609, indexed in Pubmed: 18948844.
5. Yukitake H, Takizawa M, Kimura H. Macrophage migration inhibitory factor as an emerging drug target to regulate antioxidant response element system. Oxid Med Cell Longev. 2017; 2017: 8584930, doi: 10.1155/2017/8584930, indexed in Pubmed: 28191280.
6. Bloom J, Metz C, Nalawade S, et al. Identification of iguratimod as an inhibitor of macrophage migration inhibitory factor (MIF) with steroid-sparing potential. J Biol Chem. 2016; 291(51): 26502–26514, doi: 10.1074/jbc.M116.743328, indexed in Pubmed: 27793992.
7. Yoo SA, Leng L, Kim BJ, et al. MIF allele-dependent regulation of the MIF coreceptor CD44 and role in rheumatoid arthritis. Proc Natl Acad Sci U S A. 2016; 113(49): E7917–E7926, doi: 10.1073/pnas.1612717113, indexed in Pubmed: 27872288.
8. Chen D, Xia M, Hayford C, et al. Expression of human tissue factor pathway inhibitor on vascular smooth muscle cells inhibits secretion of macrophage migration inhibitory factor and attenuates atherosclerosis in ApoE-/- mice. Circulation. 2015; 131(15): 1350–1360, doi: 10.1161/CIRCULATIONAHA.114.013423, indexed in Pubmed: 25677604.
9. Ha T, Hua F, Grant D, et al. Glucan phosphate attenuates cardiac dysfunction and inhibits cardiac MIF expression and apoptosis in septic mice. Am J Physiol Heart Circ Physiol. 2006; 291(4): H1910–H1918, doi: 10.1152/ajpheart.01264.2005, indexed in Pubmed: 16766637.

10. Chuang TY, Chang HT, Chung KP, et al. High levels of serum macrophage migration inhibitory factor and interleukin 10 are associated with a rapidly fatal outcome in patients with severe sepsis. Int J Infect Dis. 2014; 20: 13–17, doi: 10.1016/j.ijid.2013.12.006, indexed in Pubmed: 24445225.

11. Peng T, Lu X, Feng Q. Pivotal role of gp91phox-containing NADH oxidase in lipopolysaccharide-induced tumor necrosis factor-alpha expression and myocardial depression. Circulation. 2005; 111(13): 1637–1644, doi: 10.1161/01.CIR.0000160366.50210.E9, indexed in Pubmed: 15795323.

12. Su H, Na N, Zhang X, et al. The biological function and significance of CD74 in immune diseases. Inflamm Res. 2017; 66(3): 209–216, doi: 10.1007/s00011-016-0995-1, indexed in Pubmed: 27752708.

13. Dhanantwari P, Nadaraj S, Kenessey A, et al. Macrophage migration inhibitory factor induces cardiomyocyte apoptosis. Biochem Biophys Res Commun. 2008; 371(2): 298–303, doi: 10.1016/j.bbrc.2008.04.070, indexed in Pubmed: 18439909.

14. Xu X, Bucala R, Ren J. Macrophage migration inhibitory factor deficiency augments doxorubicin-induced cardiomyopathy. J Am Heart Assoc. 2013; 2(6): e000439, doi: 10.1161/JAHA.113.000439, indexed in Pubmed: 24334905.

15. Rowe MA, Harper LR, McNulty MA, et al. Reduced osteoarthritis severity in aged mice with deletion of macrophage migration inhibitory factor. Arthritis Rheumatol. 2017; 69(2): 352–361, doi: 10.1002/art.39844, indexed in Pubmed: 27564840.

16. Reinart N, Nguyen PH, Boucas J, et al. Delayed development of chronic lymphocytic leukemia in the absence of macrophage migration inhibitory factor. Blood. 2013; 121(5): 812–821, doi: 10.1182/blood-2012-05-431452, indexed in Pubmed: 23118218.

17. Zhu S, Xu T, Luo Y, et al. Luteolin Enhances Sarcoplasmic Reticulum Ca2+-ATPase Activity through p38 MAPK Signaling thus Improving Rat Cardiac Function after Ischemia/Reperfusion. Cell Physiol Biochem. 2017; 41(3): 999–1010, doi: 10.1159/000460837, indexed in Pubmed: 28222421.

18. Lin X, Sakuragi T, Metz CN, et al. Macrophage migration inhibitory factor within the alveolar spaces induces changes in the heart during late experimental sepsis. Shock. 2005; 24(6): 556–563, indexed in Pubmed: 16317387.

19. Aoki H, Kang PM, Hampe J, et al. Direct activation of mitochondrial apoptosis machinery by c-Jun N-terminal kinase in adult cardiac myocytes. J Biol Chem. 2002; 277(12): 10244––10250, doi: 10.1074/jbc.M112355200, indexed in Pubmed: 11786558.

20. White DA, Su Y, Kanellakis P, et al. Differential roles of cardiac and leukocyte derived macrophage migration inhibitory factor in inflammatory responses and cardiac remodelling post myocardial infarction. J Mol Cell Cardiol. 2014; 69: 32–42, doi: 10.1016/j.yjmcc.2014.01.015, indexed in Pubmed: 24508700.

21. Sprenkle NT, Sims SG, Sánchez CL, et al. Endoplasmic reticulum stress and inflammation in the central nervous system. Mol Neurodegener. 2017; 12(1): 42, doi: 10.1186/s13024-017-0183-y, indexed in Pubmed: 28545479.

22. Zhang C, Syed TW, Liu R, et al. Role of endoplasmic reticulum stress, autophagy, and inflammation in cardiovascular disease. Front Cardiovasc Med. 2017; 4: 29, doi: 10.3389/fcvm.2017.00029, indexed in Pubmed: 28553639.